Determinants of bistability in induction of the *Escherichia coli lac* operon

David W. Dreisigmeyer,[1] Jelena Stajic,[2,*] Ilya Nemenman,[3,2]
William S. Hlavacek,[1,2] and Michael E. Wall[3,4,2,†]

[1]*Theoretical Division*
[2]*Center for Nonlinear Studies*
[3]*Computer, Computational, and Statistical Sciences Division*
[4]*Bioscience Division, Los Alamos National Laboratory, Los Alamos, NM 87545, USA*

(Dated: July 14, 2008)

Abstract

We have developed a mathematical model of regulation of expression of the *Escherichia coli lac* operon, and have investigated bistability in its steady-state induction behavior in the absence of external glucose. Numerical analysis of equations describing regulation by artificial inducers revealed two natural bistability parameters that can be used to control the range of inducer concentrations over which the model exhibits bistability. By tuning these bistability parameters, we found a family of biophysically reasonable systems that are consistent with an experimentally determined bistable region for induction by thio-methylgalactoside (TMG) (Ozbudak et al. Nature 427:737, 2004). To model regulation by lactose, we developed similar equations in which allolactose, a metabolic intermediate in lactose metabolism and a natural inducer of *lac*, is the inducer. For biophysically reasonable parameter values, these equations yield no bistability in response to induction by lactose—only systems with an unphysically small permease-dependent export effect can exhibit small amounts of bistability for limited ranges of parameter values. These results cast doubt on the relevance of bistability in the *lac* operon within the natural context of *E. coli*, and help shed light on the controversy among existing theoretical studies that address this issue. The results also motivate a deeper experimental characterization of permease-independent transport of *lac* inducers, and suggest an experimental approach to address the relevance of bistability in the *lac* operon within the natural context of *E. coli*. The sensitivity of *lac* bistability to the type of inducer emphasizes the importance of metabolism in determining the functions of genetic regulatory networks.

INTRODUCTION

In 1957, Novick and Weiner discovered that *Escherichia coli* can exhibit discontinuous switching in expression of the *lac* operon in response to thio-methylgalactoside (TMG), with some cells expressing a large amount of β-galactosidase (β-gal), other cells expressing a small amount, and an insignificant number of cells expressing an intermediate amount [1]. Recently, this effect was further characterized using single-cell assays of fluorescence levels in a population of *E. coli* cells carrying a *lac::gfp* reporter [2]. Cells were grown overnight on sucrose in either an induced (1 mM TMG) or uninduced (no TMG) state. They were then diluted into media with defined levels of TMG and glucose; after 20 hours of growth, the cells were examined under a microscope. Under many conditions, cell populations exhibited a bimodal distribution, with induced cells having over 100 times the fluorescence level of uninduced cells. The distribution was also history-dependent: at the same final level of TMG and glucose, cells with an induced history were predominantly induced, while cells with an uninduced history were predominantly uninduced. These observations have been attributed to the existence of two steady states, i.e., bistability, in the induction of *lac* in *E. coli*.

Recent modeling studies have emphasized the importance of determining whether bistability in expression of *lac* is relevant within a natural context [3, 4, 5, 6, 7, 8]. This question remains open because experimental studies have focused on the response of *lac* expression to artificial inducers, such as TMG and isopropyl-β, D-thiogalactopyranoside (IPTG), rather than the natural inducer, allolactose. This difference is critical because artificial inducers (also known as gratuitous inducers) are not metabolized by the induced enzyme, whereas the natural inducer is a metabolic intermediate in lactose degradation, which is catalyzed by the induced enzyme.

Savageau [3] found important differences between induction by IPTG vs. lactose in his theoretical treatment of bistability in the *lac* operon. In Savageau's model, because production and decay of allolactose are both proportional to the β-gal concentration, bistability is forbidden. Expression of *lac* in response to lactose was therefore predicted not to exhibit bistability. This prediction agreed with the absence of *steady-state* bistability in an experimental study of populations of *E. coli* cells exposed to lactose, described in the Supplementary Material of Ref. [2]—in that study, only *transient* bimodal distributions of green fluorescence levels among cells were observed at some glucose concentrations. It was later noted that models with operon-independent decay of lactose (e.g., due to dilution by cell growth) could exhibit bistability [7]. Several studies using

such models found either a bistable or graded response to lactose, depending on parameter values or external glucose levels [5, 6, 7, 8, 9, 10], and, in agreement with the model of Savageau, a model of van Hoek & Hogeweg [7] was explicitly shown to exhibit no bistability in the absence of operon-independent decay of allolactose. However, these studies disagree in their assessment of whether bistability is present [5, 6, 10] or absent [7, 8, 9] in expression of *lac* among *E. coli* cells in a natural context.

In addition to predicting whether *lac* induction exhibits bistability, some studies have addressed the question of whether bistability might enhance or hinder the performance of *E. coli* cells. Both Savageau [4] and van Hoek & Hogeweg [9] found that bistability increases the time required to respond to sudden increases in environmental lactose, which can be a disadvantage in competition for nutrients. These results argue against the natural relevance of bistability in *lac* expression.

Another important question that has not yet been addressed is whether the experimental observations of bistability in Ref. [2] are consistent with independent biophysical data that characterize processes relevant to regulation of *lac* expression. Although phenomenological models were developed to reproduce the steady-state behavior [2] and the experimentally characterized dynamics of switching between stable steady states [11], these models were not constrained by independent biophysical data. For example, it is unclear whether the phenomenological models are consistent with independently measured permease transport kinetics. On the other hand, studies of bistability using more detailed, biophysical models of *lac* induction were either only partially constrained [7] or did not consider the response to artificial inducers [5, 6, 10].

Here we analyze bistability in ordinary differential equation (ODE) models of *lac* induction. We use ODEs because we restrict our analysis to steady-state behaviors, and because the protein concentrations in fully induced cells are O(10^4) per cell (see Parameter Values section) and have negligible fluctuations. Similar equations describe induction by artificial inducers or lactose; however, the models for the two types of inducers are topologically distinct and one cannot be obtained as a limiting case of the other. We first use the artificial induction model to gain insight into key determinants of bistability of *lac* expression in response to TMG, and to understand how characteristics of bistability are controlled by model parameters. We then use the resulting insight to tune the parameters of the model to match the bistable behavior observed by Ozbudak et al. [2], and to predict mechanisms by which bistability might be abolished. Finally, like previous modeling studies, we use the closely related lactose induction model to address the question of whether *lac* expression might be bistable in a natural context, contributing to resolution of what is

now a long-standing controversy.

MODEL

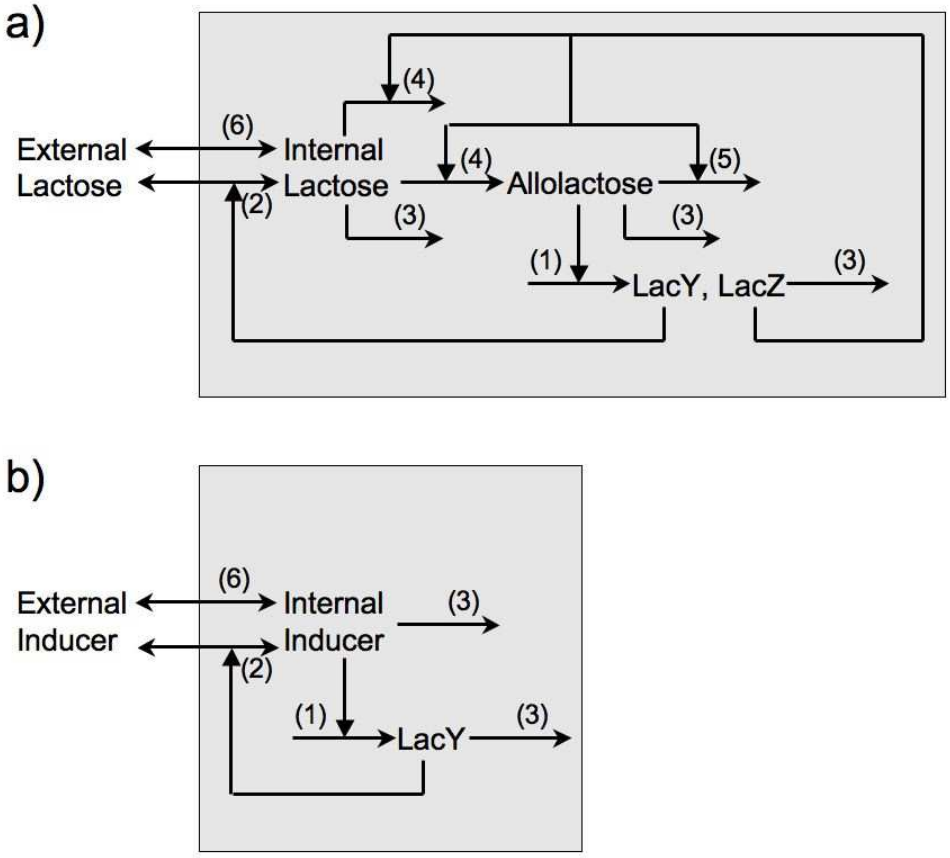

FIG. 1: Circuitry for models of *lac* induction. a) Model for induction by lactose (Eqs. (1)), including the following processes: (1) proportional production of permease (LacY) and β-gal (LacZ); (2) permease-mediated transport of lactose; (3) dilution of intracellular species by cell growth; (4) β-gal catalyzed degradation of lactose, producing both the metabolic intermediate allolactose, and the ultimate products of degradation, glucose and galactose; (5) β-gal catalyzed degradation of allolactose, producing glucose and galactose; and (6) passive transport of inducer. b) Model for induction by artificial inducers (Eqs. (2)), including: (1) proportional production of permease (LacY) and β-gal (LacZ); (2) permease-mediated transport of inducer; (3) dilution of intracellular species by cell growth and (6) passive transport of inducer.

In our model of *lac* induction (Fig. 1a), the following set of coupled ordinary differential equations relate the internal lactose concentration (l), allolactose concentration (a), and β-galactosidase

concentration (z) to the external lactose concentration (l^*)

$$\dot{l} = \alpha_0 (l^* - l) + \alpha z \frac{(l^* - \phi\rho l)}{K_i + l^* + \rho l} - \frac{\beta z l / K_{m,l}}{1 + a/K_{m,a} + l/K_{m,l}} - \gamma l, \tag{1a}$$

$$\dot{a} = \frac{\nu\beta z l / K_{m,l}}{1 + a/K_{m,a} + l/K_{m,l}} - \frac{\delta z a / K_{m,a}}{1 + l/K_{m,l} + a/K_{m,a}} - \gamma a \text{ and} \tag{1b}$$

$$\dot{z} = c\gamma + \frac{\epsilon\gamma a^n}{K_z^n + a^n} - \gamma z. \tag{1c}$$

In Eqs. (1), α and K_i are the rate constant and Michaelis constant for permease-dependent lactose import, $\phi\alpha$ and $\rho^{-1}K_i$ are the rate constants for permease-dependent lactose export, β and $K_{m,l}$ are the rate constant and Michaelis constant for lactose degradation, ν is the branching fraction of lactose degradation to allolactose, δ and $K_{m,a}$ are the rate constant and Michaelis constant for allolactose degradation, γ is the rate of dilution due to cell growth, $c\gamma$ and $\epsilon\gamma$ are the basal and inducible rates of β-galactosidase production, K_z is the allolactose concentration at half-maximal induction of β-galactosidase production, and n is the Hill number for lactose induction of β-galactosidase production. The metabolic flux terms in Eqs. (1) (β and δ terms) include the effects of competition between allolactose and lactose for access to β-galactosidase; they are derived from mass-action kinetic equations by assuming fast partitioning of enzyme among the free, lactose-bound, and allolactose-bound states.

The model of permease-dependent transport is consistent with the kinetic scheme described in Ref. [12], in which permease switches between inward-binding and outward-binding conformations, and accepts substrate from either the interior or exterior of the cell depending on the conformation. Similar to the enzyme flux terms, the transport term in Eq. (1a) (α term) is derived from mass-action kinetic equations by assuming fast partitioning of permease among its various states. Active transport ($\phi < 1$) occurs through co-transport of substrate with a proton (symport), and is powered by a proton gradient across the membrane. The transport model is supported by crystallography studies [13, 14]. Changes in interior and exterior pH, membrane potential, and the equilibrium constant between inward- and outward-facing conformations are considered implicitly through changes in kinetic parameters; we assume these conditions are not influenced by changes in substrate concentration. We note that Ref. [12] considered a limiting case (exchange) in which switching between the two conformations is only kinetically accessible when substrate is bound to the permease, and both active transport and efflux are blocked. Here we consider more general equations in which all transitions in the model are allowed; our transport equation therefore differs

from that in Ref. [12].

To focus on the operating conditions of the system that are most relevant to lactose utilization by *E. coli*, we only consider regulation in the absence of glucose. This focus is appropriate because, in the presence of glucose, *lac* is not essential for growth, and induced β-galactosidase levels are low [15].

Similarly, the model of artificial induction of *lac* (Fig. 1b) is given by

$$\dot{l} \;=\; \alpha_0 \left(l^* - l\right) + \alpha z \frac{\left(l^* - \phi\rho l\right)}{K_i + l^* + \rho l} - \gamma l \;\; \text{and} \tag{2a}$$

$$\dot{z} \;=\; c\gamma + \frac{\epsilon\gamma l^n}{K_z^n + l^n} - \gamma z. \tag{2b}$$

In Eqs. (2), variables and parameters have the same meaning as in Eqs. (1), except l and l^* correspond to the level of internal and external artificial inducer (e.g., IPTG or TMG), respectively, and α_0 is the rate constant for permease-independent passive transport across the membrane.

In Eqs. (1) and Eqs. (2), protein expression is lumped with gene expression, and the dependence of promoter activity on the level of signal (TMG or allolactose) is modeled using a simple Hill function, which is significantly simpler than other models [5, 6, 7, 8, 9, 10, 16, 17]. On the other hand, Eqs. (1) consider the effects of competition among substrates in permease transport and metabolic processes, unlike other models of *lac* induction [2, 3, 4, 5, 6, 7, 9, 10, 16, 18]. Compared to the model of Savageau [3, 4], Eqs. (1) consider operon-independent decay of allolactose, without which bistability in response to lactose is impossible [3, 4, 7], as discussed above. Overall, Eqs. (1) and Eqs. (2) are less detailed than the *lac* induction models used in Refs. [16], [5], [6], [7], [9], and [10], and are more detailed than those used in Refs. [3], [4], [18], and [2], and they therefore constitute intermediate complexity equations describing *lac* induction. Compared to the simpler models, the intermediate level of detail provides increased contact between model parameters and biophysical measurements, and compared to more detailed models, it facilitates analysis of the equations and interpretation of the results.

PARAMETER VALUES

We used the parameter values and ranges listed in Table I to analyze bistability in Eqs. (1) and Eqs. (2). The values in the table were obtained as follows:

- γ. We assume the doubling time under the conditions in Ref. [2] is 30-60 min. We note,

however, that this time might be very different for *E. coli* growing under stress in the gut or aqueous environment; this represents a source of uncertainty concerning the biological relevance of our predictions.

- α_0. Experimental data on passive transport of inducers seems scarce in the literature. Ref. [19] reports a measured rate constant of 0.14 min^{-1} for TMG, and Ref. [20] reports permease-independent efflux rate constants of 0.022 min^{-1} and 0.054 min^{-1} for lactose measured under conditions of deinduction and induction, respectively. However, the TMG value was obtained using competitive inhibition of permease using an undescribed method, and the lactose values were obtained using a model of lactose flux that is inconsistent with the mechanism in Ref. [12], and that ignores dilution by cell growth. We therefore consider the above values to be uncertain. Here we explore the same range as that used in the modeling study described in Ref. [9], which encompasses the above values. We analyze the lactose system using a nominal value of 0, allowing for the possibility that the actual value might be very small; this value also maximizes the potential for bistability.

- α. An approximate range of 1-100 s^{-1} for sugar transport turnover numbers was obtained from the review by Wright et al. [21]. The range is broader than measured values [22] because measurements were made at 25°C rather than at the physiological temperature of 37°C in the host environment of the gut, and at which measurements in Ref. [2] were performed. Turnover numbers can vary by about an order of magnitude depending on the membrane potential and proton gradient [22], leading to additional uncertainty. The nominal value of $600\ \text{min}^{-1}$ is consistent with Ref. [22] assuming the production rate of functional permease is about the same as that of functional β-gal. Because permease is a monomer while β-gal is a tetramer, this assumption entails a four-fold smaller synthesis rate for permease monomers compared to β-gal subunits. This seems possible, as (1) galactoside acetyltransferase (GATase) monomer synthesis is eight-fold smaller than β-gal subunit synthesis; (2) due to incomplete operon transcription and the order of genes in the operon (*lacZYA*), the amount of mRNA transcribed from the GATase gene (*lacA*) and permease gene (*lacY*) is smaller than that from the β-gal gene (*lacZ*); (3) there is some evidence that permease monomers are made in smaller amounts than β-gal subunits [23].

- ϕ. The nominal value of 0.5 was obtained by comparing the active transport and efflux turnover numbers in Ref. [22], Table 1. Because permease transport kinetics are sensitive to

membrane potential and proton gradient [22], we allow the value to decrease in the search for bistable conditions (we found that bistability is abolished for higher values of ϕ).

- K_i. A nominal value of 0.5 mM was obtained from Ref. [22]. The range was applied as per α, and encompasses measured values [22, 24, 25].

- ρ. Guided by Ref. [22], Table 1, we assume that the Michaelis constant for permease-dependent import can be up to 10 times smaller than that for export. The nominal value of 0.1 is consistent with the smallest in that table, and yields the greatest potential for bistability in the lactose system.

- β. A total lactose turnover number for β-galactosidase of 2.85×10^4 min^{-1} is estimated from a measured value of $V_{max} = 61.3$ μM min^{-1} mg^{-1} in Ref. [26]. This estimate is an order of magnitude greater than the value 3.6×10^3 min^{-1} given in Ref. [27], but the two estimates agree closely when one considers that β-gal converts about half of its lactose substrate to glucose and galactose, rather than allolactose, and that the enzyme is composed of four monomeric catalytic subunits. The estimate given in Ref. [27] is appropriate for total turnover of lactose on a per monomer basis. Like for α, because measurements were performed at 30°C, we consider a range of values ten times lower to ten times higher than the nominal value.

- $K_{m,l}$. The nominal value was obtained directly from Ref. [28]. As for β, because of temperature considerations, we use a range from ten times lower to ten times higher than the nominal value.

- ν. The value $\nu = 0.468$ was calculated from the total rate of β-gal degradation of lactose and the partial flux from lactose to allolactose reported in Ref. [26]. We take it to be a constant because the ratio of reaction products was found to be insensitive to temperature changes between 30°C and 0°C.

- δ. An allolactose turnover number for β-gal of 2.3×10^4 min^{-1} is estimated from a measured value of $V_{max} = 49.6$ μ mol min^{-1} mg^{-1} in Ref. [28]. As for β, because of temperature considerations, we use a range from ten times lower to ten times higher than the nominal value.

- $K_{m,a}$. The nominal value was obtained directly from Ref. [28]. As for β, because of temperature considerations, we use a range from ten times lower to ten times higher than the nominal value.

- ϵ. Using a production rate of 5 β-gal tetramers per cell per second for a 48 min generation time [29], 14,400 molecules are produced during a generation at full induction–this is the number of molecules in the cell after doubling (supporting our choice of a noiseless model). Assuming a 1 $\mu\mathrm{m}^3$ mean cell volume [30] and linear volume increase in time [31], the volume after doubling is approximately 0.7 $\mu\mathrm{m}^3$, leading to a concentration of 34,286 nM.

- c. This value is derived from ϵ, assuming a 1000-fold increase in β-galactosidase levels upon induction [32].

- K_z and n. These values are estimated from IPTG induction data in permease knockout cells both from Ref. [33], Fig. 15 and from data compiled in Ref. [34], Figs. 1 and 2. The nominal value $n = 2$ was estimated from the slopes of the curves in the figures, and K_z was determined by estimating from the figures the concentration of IPTG at half-maximal induction. The nominal value of 10^5 nM was estimated from data compiled in Ref. [34]. To determine the range, an approximate lower value of 10^4 nM was obtained from Ref. [33], and we allowed for an upper value of 10^6 nM to account for potential differences between induction by IPTG and TMG or lactose.

RESULTS

We first used Eqs. (2) to determine how parameter values control bistability in the steady-state response of *lac* expression to artificial inducers. To detect and characterize bistability for a given set of parameter values, we solved for $z(l)$ and $l^*(l)$ as rational functions of l. Bistability in *lac* expression exists when the line describing steady-state levels of z vs. l^* adopts a characteristic "S" shape, as shown in Fig. 2. Within the bistable range of l^*, the highest and lowest levels of z are stable steady-state solutions and the intermediate level of z is an unstable steady-state solution of Eqs. (1). The bistable range is defined by the lower ($l^* = L$) and upper ($l^* = U$) turning points, as illustrated in Fig. 2. An analogous signature of bistability can be seen in examining steady-state

TABLE I: Parameter values. Nominal values are those used to generate the lactose induction curves in Fig. 8.

Param	Description	Nominal	Range
γ	growth rate	–	$0.0116\ \mathrm{min}^{-1}$ – $0.0231\ \mathrm{min}^{-1}$
α_0	passive transport rate constant	0	0 – $1.35\ \mathrm{min}^{-1}$
α	permease import turnover number	$600\ \mathrm{min}^{-1}$	$6 \times 10^1\ \mathrm{min}^{-1}$ – $6 \times 10^3\ \mathrm{min}^{-1}$
ϕ	ratio of permease export to import turnover numbers	0.5	0 – 0.5
K_i	permease Michaelis constant	5×10^5 nM	5×10^4 nM – 5×10^6 nM
ρ	ratio of permease import to export Michaelis constants	0.1	0.1 – 1
β	β-gal lactose turnover number	$2.85 \times 10^4\ \mathrm{min}^{-1}$	$2.85 \times 10^3\ \mathrm{min}^{-1}$ – $2.85 \times 10^5\ \mathrm{min}^{-1}$
ν	lactose$\rightarrow$ allolactose β-gal branching fraction	0.468	–
$K_{m,l}$	β-gal lactose Michaelis constant	2.53 mM	0.253 mM – 25.3 mM
δ	β-gal allolactose turnover number	$2.30 \times 10^4\ \mathrm{min}^{-1}$	$2.30 \times 10^3\ \mathrm{min}^{-1}$ – $2.30 \times 10^5\ \mathrm{min}^{-1}$
$K_{m,a}$	β-gal allolactose Michaelis constant	1.2 mM	0.12 mM –12.0 mM
ϵ	fully induced β-gal level	34285 nM	–
c	basal β-gal level	34.3 nM	–
K_z	signal level at half-maximal *lac* induction	10^5 nM	10^4 nM – 10^6 nM
n	Hill number for signal-dependent *lac* induction	2	–

levels of l vs. l^* (not shown). For a model with given parameter values, L and U can be located by finding the roots of either dl^*/dz or dl^*/dl using an eigenvalue solver.

We analyzed Eqs. (2) for systems with $\alpha_0 = 0$ and $\phi = 0$, $\rho = 1$, $n = 2$, and all other sets of parameter values drawn from the ranges in Table I. Sets of 100 values each for K_i and K_z were obtained using logarithmically even sampling over their allowed ranges. Because the steady-state

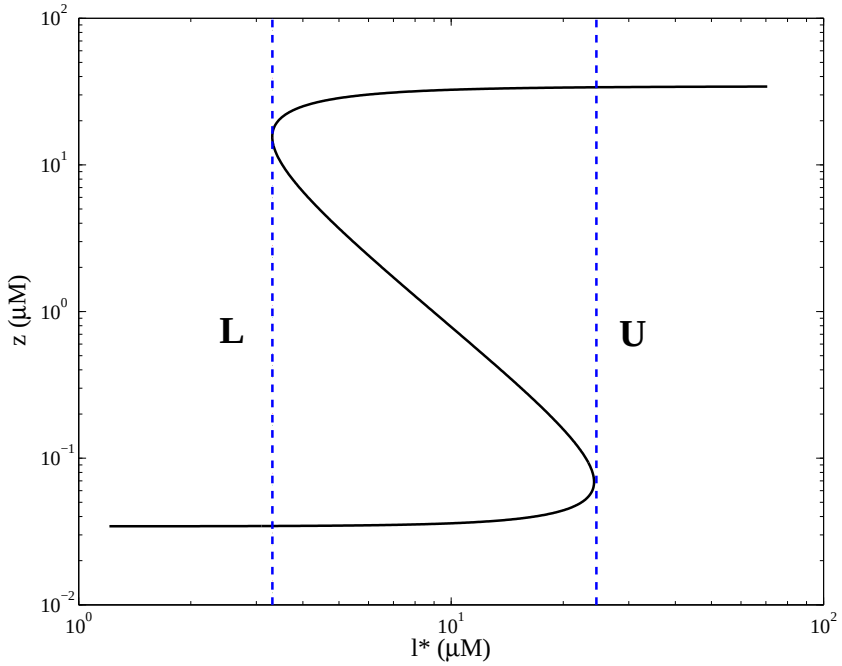

FIG. 2: An example of bistable behavior in the artificial induction model (Eqs. (2)). The upper (U) and lower (L) turning points are consistent with the experimental results in Ref. [2]. The parameter values are $\gamma = .0231\ \mathrm{min}^{-1}$, $\alpha = 60\ \mathrm{min}^{-1}$, $K_z = 123,285$ nM and $K_i = 1,077,217$ nM.

solutions of Eqs. (2) only depend on α and γ through the ratio α/γ, rather than sampling α and γ individually, we obtained 100 values of α/γ using logarithmically even sampling between the upper and lower bound computed from Table I. This sampling scheme yielded $100 \times 100 \times 100 = 10^6$ systems with different values of $(\alpha/\gamma, K_i, K_z)$.

We found that all 10^6 systems exhibited some degree of bistability in response to induction by artificial inducers. The dependence of the range of bistability on model parameters was further analyzed using two measures that we introduce here: the ratio U/L, and the product UL. We used these measures to estimate the percentage of systems for which bistability might be observable in an experiment like that in Ref. [2]. By inspecting the measurement errors in Ref. [2], we estimate that systems with $U/L > 1.1$ and $UL > 0.01\ \mu\mathrm{M}^2$ exhibit bistability that is favorable for experimental observation, and that systems with either $U/L < 1.1$ or $UL < 0.01\ \mu\mathrm{M}^2$ exhibit bistability that is unfavorable for experimental observation. Among systems with parameter values sampled as described above, by these criteria, experimental observation of bistability is favorable for 65% of systems, and unfavorable for 35% of systems.

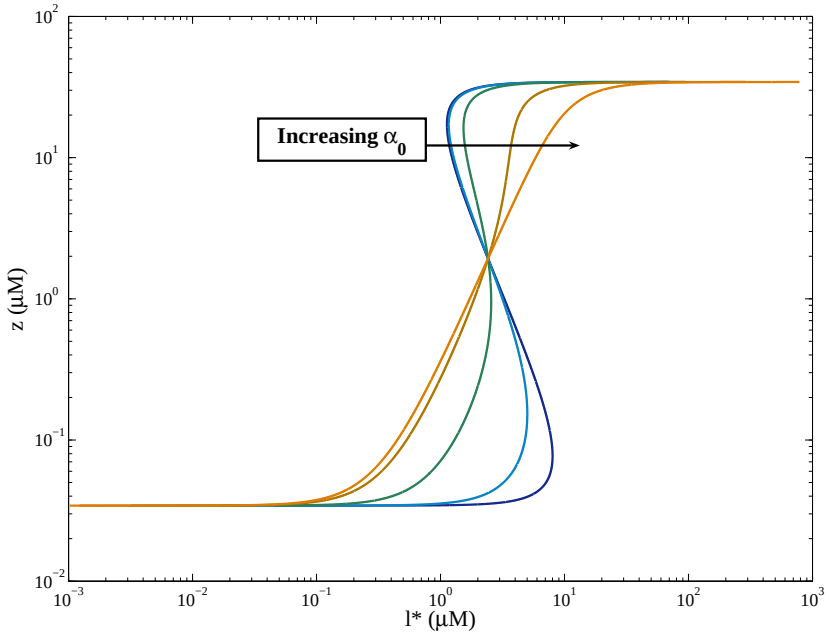

FIG. 3: Effects of variations in the $\alpha_0 > 0$ parameter on an artificially induced system with $\phi = 0\ \mathrm{min}^{-1}$ and $\alpha_0 = 10^{-k}\ \mathrm{min}^{-1}$, $k = 0, \ldots, 4$. The other parameters are given by $n = 2,\ \gamma = .0231\ \mathrm{min}^{-1},\ \epsilon = 34286\ \mathrm{nM},\ c = 34.3\ \mathrm{nM},\ K_i = 5 \times 10^6\ \mathrm{nM},\ K_z = 10^4\ \mathrm{nM}$ and $\alpha = 60\ \mathrm{min}^{-1}$.

To compare Eqs. (2) to the data in Ref. [2], we first selected a subset of systems for which the bistable region is in the same neighborhood as that in Ref. [2]: from $3\ \mu$M to $30\ \mu$M TMG. Considering this range, out of the 10^6 systems sampled, we selected 187,108 systems for which $L > 1\ \mu$M and $U < 100\ \mu$M for further analysis. Interestingly, we found that all of these systems collapse to a single curve when displayed in the space of $\log_{10}(U/L)$ vs. $\log_{10}(K_i/K_z)$ (Fig. 5), indicating that U/L can be precisely tuned using the parameter $X = K_i/K_z$. As shown in Fig. 5, the dependence was accurately modeled using the equation

$$\log_{10}(U/L) \ \approx \ \frac{(K_i/K_z)^{.93}}{(K_i/K_z)^{.93} + (.27)^{.93}} - \frac{1}{10} \geq 0. \tag{3}$$

Next, we found that, at a given value of $X = K_i/K_z$, without changing the value of U/L, UL could be tuned precisely using the parameter $Y = K_i K_z \gamma/\alpha$. As shown in Fig. 6, this dependence was accurately modeled using the equation

$$\log_{10}(UL) \ = \ C_0(X) + C_1(X) \log_{10}(Y). \tag{4}$$

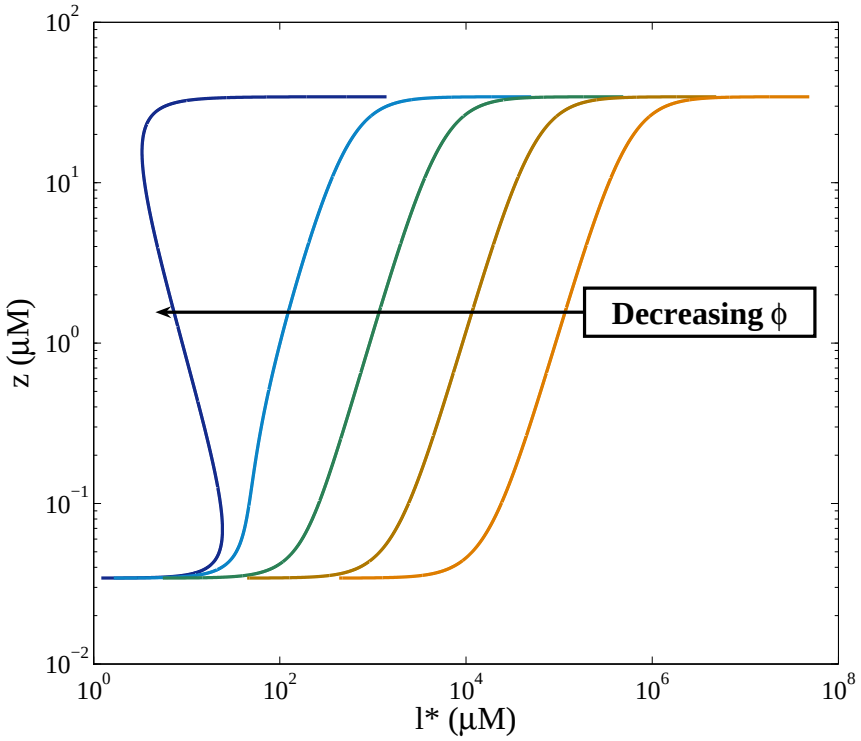

FIG. 4: Effects of variations in the $\phi > 0$ parameter on an artificially induced system with $\alpha_0 = 10^{-4}\ \mathrm{min}^{-1}$ and $\phi = 0$ and $10^{-k}\ \mathrm{min}^{-1}$, $k = 1, \ldots, 4$. The other parameter values are as in Fig. 3.

Figure 7 shows the X-dependence of the parameters $C_0(X)$ and $C_1(X)$, obtained numerically using systems with similar values of X. For the range of systems considered here, we found that $C_0(X)$ could be fit using a third order polynomial in $\log_{10}(X)$, and that $C_1(X)$ could be taken as a constant.

We used Eq. (3) and Eq. (4) to obtain a family of systems that are consistent with the parameter values in Table I and that exhibit a range of bistability consistent with that observed in Ref. [2], with $\log_{10}(U/L) \approx .86$ and $\log_{10}(UL) \approx 1.92$. An example of the steady-state behavior of one such system is illustrated in Fig. 2.

Increasing either α_0 or ϕ above zero tends to reduce or abolish bistability in artificially induced systems. As α_0 is increased (Fig. 3), first U begins shifting to lower values of l^*, then L begins shifting to higher values of l^*, leading to an asymptotic behavior in which bistability is abolished. Like changes in α_0, as ϕ is increased (Fig. 4), L shifts to higher values of l^*; however, by contrast, U does not initially show a significant change. As ϕ is increased further, the entire induction curve begins to shift to higher levels of l^*.

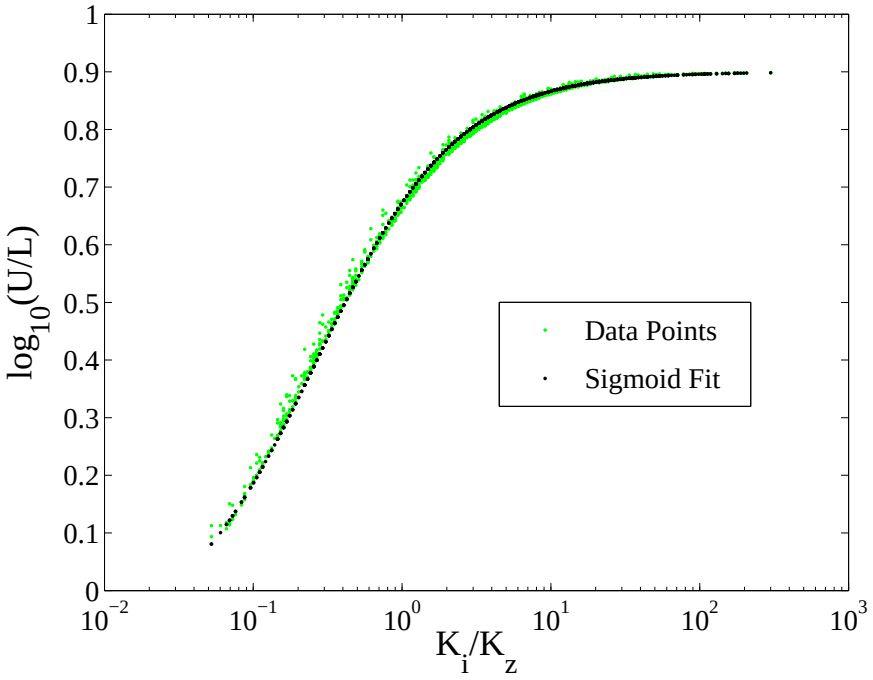

FIG. 5: Relation between U/L and the parameter $X = K_i/K_z$. Data points are generated using the artificial induction model (Eqs. (2)) with parameter values selected as described in the text. Points with $L > 1\mu$M and $U < 100\mu$M were selected; shown are a subset of points that illustrate the general trend, which is described well using Eq. (3).

We then considered systems with $\rho < 1$. Using Eqs. (2), we found that the steady-state behavior of such systems is equivalent to that of systems with $\rho = 1$ under the transformation

$$l \rightarrow \rho l, \tag{5a}$$

$$K_z \rightarrow \rho K_z, \text{ and} \tag{5b}$$

$$\gamma \rightarrow \frac{\gamma}{\rho} + (1-\rho)\frac{\alpha_0}{\rho} \tag{5c}$$

Because both K_i/K_z and $K_iK_z\gamma/\alpha$ increase under this transformation, we expected bistability to be enhanced in systems with $\rho < 1$ (see Figs. 5 and 6). Indeed, we found that bistability in systems with $\rho < 1$ exhibited a higher tolerance to increases in α_0 and ϕ: for example, the system with $K_z = 10$ μM, $K_i = 5$ mM, $\alpha = 890$ min^{-1}, $\phi = 0.1$, $\alpha_0 = 10^{-3}$ min^{-1}, and $\rho = 0.1$ exhibits bistability with $\log_{10}(U/L) = 0.85$ and $\log_{10}(UL) = 1.91$, which is consistent with the data in Ref. [2].

We used similar methods to analyze Eqs. (1) which describe induction by lactose. Like the

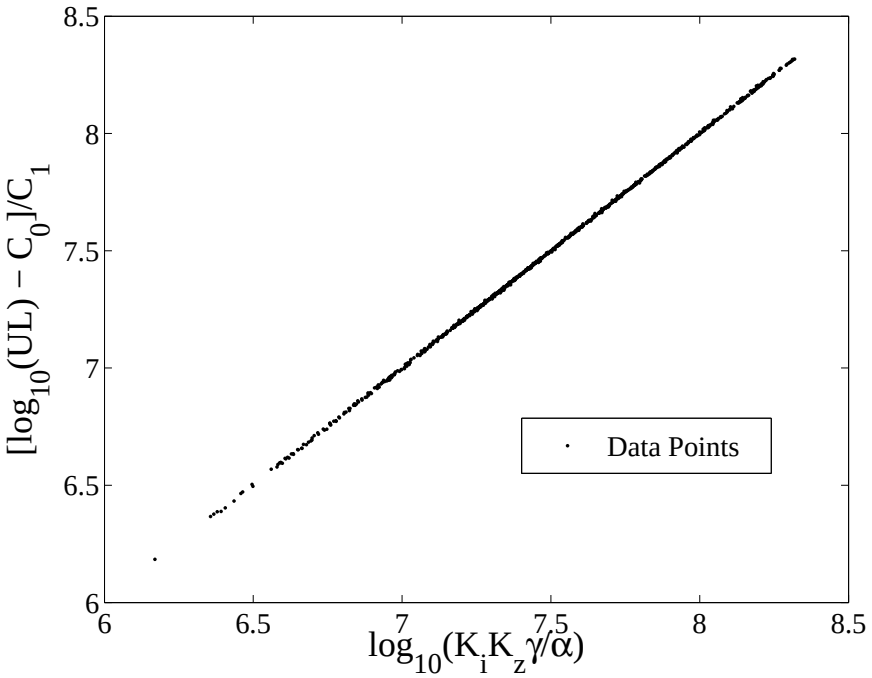

FIG. 6: Relation between the bistability measure UL and the parameter $Y = K_i K_z \gamma/\alpha$. Using the coefficients C_0 and C_1 (Fig. 7) as indicated on the y-axis yields a linear relation that is well-modeled using Eq. (4). The data points are generated as described in Fig. 5 and in the text.

artificial induction model, the steady-state behavior of systems with $\rho < 1$ is equivalent to that of systems with $\rho = 1$ under the transformations in Eqs. (5), with the additional re-scaling

$$K_{m,l} \rightarrow \rho K_{m,l}. \tag{6}$$

No bistability was present in the system with nominal parameter values from Table I with $\phi = 0.5$ (Fig. 8), which is consistent with the theory of Savageau [3] and the Supplementary Material of Ref. [2]. However, guided by the results for artificial inducers in Fig. 4, we examined systems with $\phi = 0$. Although the system with otherwise nominal parameter values did not exhibit bistability, other systems that have parameter values consistent with the ranges in Table I did exhibit bistability. We located the system that exhibits the largest values of U/L and UL; for this case, α, β, δ, ρ and K_z assume their lowest values in Table I while γ, $K_{m,l}$, $K_{m,a}$ and K_i assume their highest values (Fig. 9).

To estimate the distribution of systems exhibiting the different qualitative behaviors, as for the case of artificial inducers, we analyzed 10^5 systems with randomly sampled parameter values, all

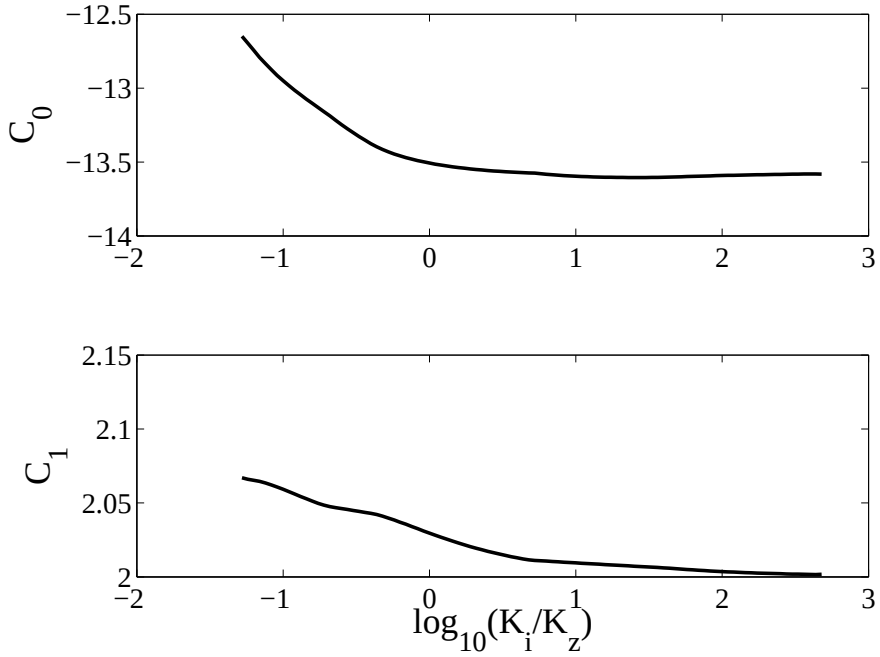

FIG. 7: Dependence of the coefficients for the UL regression model in Eq. (4) on $X = K_i/K_z$. By allowing C_0 and C_1 to depend on X, the bistability measure UL has a simple linear relationship with $Y = K_i K_z \gamma/\alpha$ (Fig. 6). The value of X is determined by Eq. (3) for a given value of U/L (Fig. 5).

with $\phi = 0$ and $\rho = 0.1$. We found that 99.82% of these systems exhibit no bistability, 0.07% exhibit bistability favorable for observation ($U/L > 1.1$ and $UL > 0.01$ μM^2), and 0.11% to exhibit bistability that is unfavorable for observation ($U/L < 1.1$ or $UL < 0.01$ μM^2). These statistics are virtually unchanged for systems with $\rho = 1$. Increasing ϕ to even a small fraction of its nominal value rapidly abolishes bistability for all combinations of other parameter values in Eqs. (1) (Fig. 10).

DISCUSSION

For the equations describing induction by artificial inducers, we found that the range of external inducer concentrations over which systems with $\alpha_0 = 0$ and $\phi = 0$ exhibit bistability is precisely controllable by two rational combinations of model parameters. First, the value of U/L can be specified by choosing a value of the parameter $X = K_i/K_z$ using Eq. (3). Then, using this value of X, the value of UL can be specified by choosing a value of the parameter $Y = K_z K_i \alpha/\gamma$ using Eq. (4) and the empirically determined $C_0(X)$ and $C_1(X)$ (Fig. 7). By adjusting these parameters,

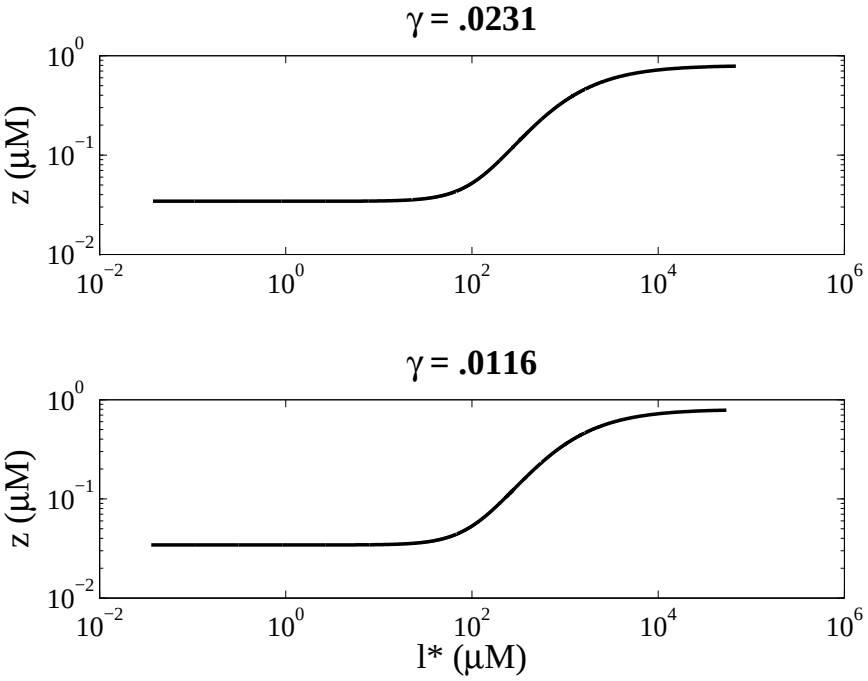

FIG. 8: Lactose induction behavior calculated using the nominal values in Table I. Neither the system with $\gamma = 0.231\ \mathrm{min}^{-1}$ (top) nor the system with $\gamma = 0.116\ \mathrm{min}^{-1}$ (bottom) exhibits bistability.

we were able to demonstrate agreement with the bistable range for TMG induction from Ref. [2].

Small increases in α_0 and ϕ abolished bistability in artificially induced systems with $\rho = 1$. Bistability was less sensitive to increases in α_0 and ϕ in systems with $\rho = 0.1$; however, even with $\rho = 0.1$, bistability was abolished in systems with α_0 as high as $0.01\ \mathrm{min}^{-1}$. This value is smaller than measured permease-independent diffusion rates for TMG [19] and lactose [20]; combined with uncertainty in these measurements (Parameter values), this discrepancy motivates further studies of permease-independent diffusion of *lac* inducers.

To achieve agreement with the bistable range of roughly $3\ \mu\mathrm{M}$ to $30\ \mu\mathrm{M}$ in Ref. [2], c and ϵ in Eqs. (2) were tuned to exhibit a 1000-fold induction of protein expression. While this value is reasonable based on previous studies, at first glance, it appears to disagree with the roughly 100-fold induction of GFP expression reported in Ref. [2]. Indeed, we analyzed systems with alternative values of c and ϵ that yield 100-fold induction, and none of them exhibited bistable ranges that agree with the range reported in Ref. [2]. However, the $lac :: gfp$ reporter used in Ref. [2] begins at -84 with respect to the start site, and extends to +20; it therefore seems to be missing all of the O2 sequence, and some of the O3 sequence. Such a difference could easily lead

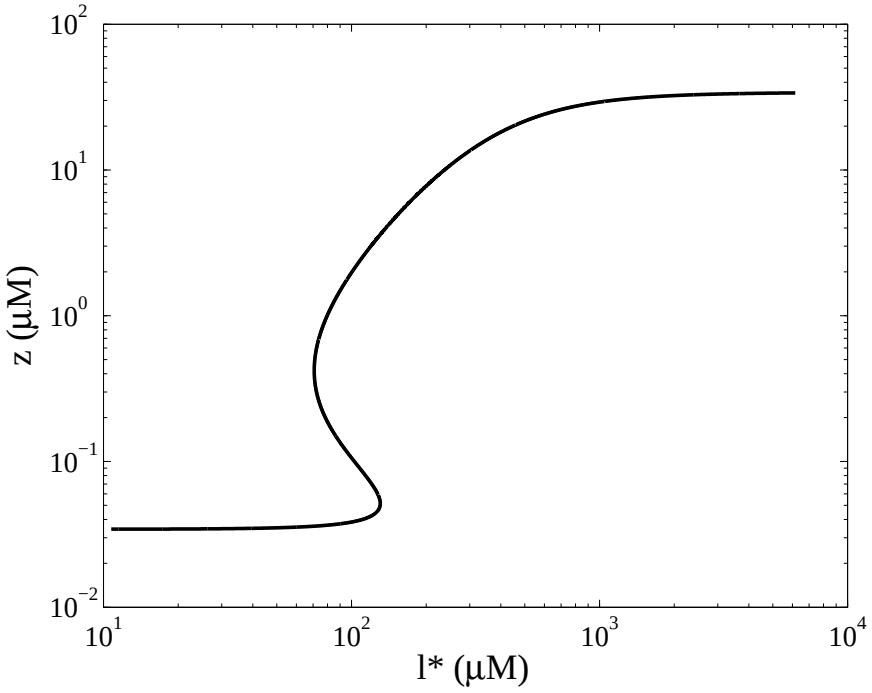

FIG. 9: Bistability in the $\phi = 0$ lactose-induced system with α, β, δ, ρ, and K_z at their lowest values in Table I and γ, $K_{m,l}$, $K_{m,a}$, and K_i at their highest values. This is the system that exhibits the largest values of U/L and UL within the allowed ranges of parameter values.

to a 10-fold difference in induction of the reporter compared to the native *lac* promoter; evidence for such an effect could be sought experimentally, e.g. by calibrating the fluorescence levels against measurements of β-gal activity.

The curve in Fig. 9 illustrating an extreme example of bistability in response to lactose for $\phi = 0$ closely resembles a similar curve shown in van Hoek & Hogeweg [7], Fig. 2B. Thus, although our model is less detailed than theirs, it can exhibit comparable steady-state behavior. In addition, Ref. [9] considered a stochastic model of *lac* induction, and Ref. [8] considered a more detailed model of the dependence of promoter activity on the level of inducer that includes DNA looping; nevertheless, like the present study, Refs. [7, 8, 9] each reported a lack of bistability in lactose induction of *lac*. These consistencies lend support to our choice of an intermediate complexity model of bistability in *lac*.

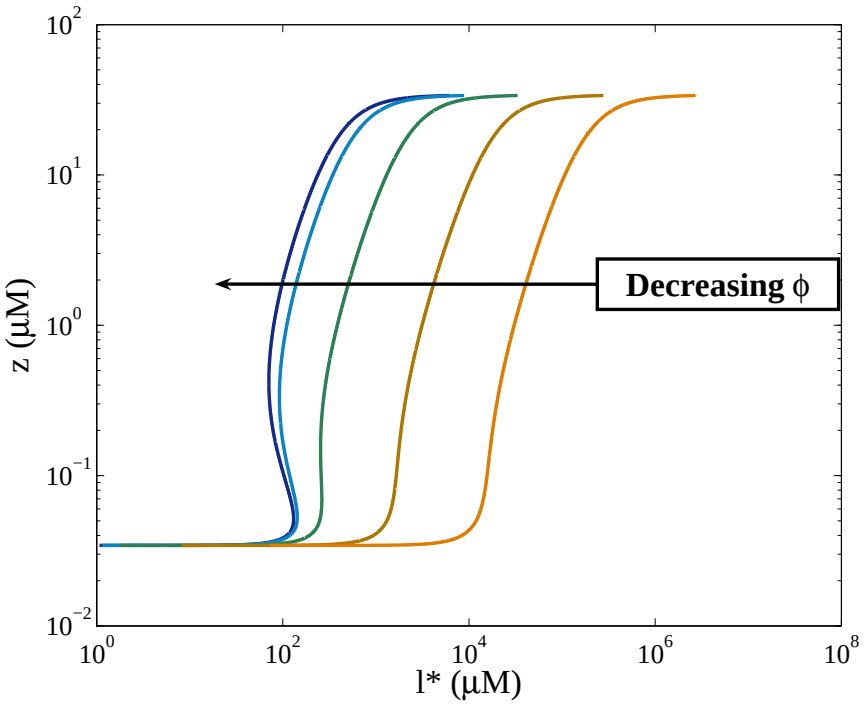

FIG. 10: Influence of ϕ on bistability in lactose induction. The leftmost curve corresponds to the same system illustrated in Fig. 9, except with $\rho = 1$ (the two are nearly identical). The curves to the right correspond to the same systems, except $\phi = 10^{-k}\ \mathrm{min}^{-1}$, $k = 1, \ldots, 4$. Bistability in lactose induction is abolished even for small values of ϕ.

CONCLUSIONS

The lack of bistability observed for induction by lactose agrees with modeling studies concluding that bistability in *lac* expression is irrelevant to *E. coli* in a natural context [3, 4, 7, 8, 9]. Thus, although bistable behavior in *lac* is now well-documented [1, 2, 35], because it has only been experimentally observed using artificial inducers, its relevance within the natural context of *E. coli* is doubtful. Indeed, it is surprising that the *lac* operon has been considered to be a paradigm of bistability in gene regulation, considering the gaps in understanding that remain after so many careful experimental and theoretical studies.

The present results predict that bistable behavior can be promoted by (1) hindering the kinetics of permease transport (α, K_i) and β-gal catalysis (β, δ, $K_{m,l}$, $K_{m,a}$); (2) lowering the required level of allolactose for half-maximal *lac* expression (K_z); (3) accelerating cell growth (γ); and (4) decreasing the Michaelis constant for permease influx relative to that for efflux (ρ). These predictions suggest genetic targets for engineering *E. coli* strains that exhibit a clear signature of

bistability. Experiments to compare the behavior of such strains with wild-type cells would help to clarify whether bistability in *lac* expression is relevant in a natural context.

Here, we found that metabolic fluxes are key determinants of bistability in *lac* induction, and that the qualitative behavior of the system can change depending on metabolism of of inducers. Previously, we found that diversity in the interaction of an input signal with transcription factors leads to diversity in the qualitative behavior of a feed-forward loop gene circuit [36]. We expect these findings to apply broadly to genetic regulatory systems in *E. coli* and other organisms. Overall, the results of these studies emphasize the importance of the nature of the input signal in determining the functions of genetic regulatory circuits.

We thank Michael A. Savageau for discussions, and Atul Narang for reading the manuscript. This work was supported by the US Department of Energy through contract DE-AC52-06NA25396, and grant GM 80216 from the National Institutes of Health. The collaboration was facilitated by the First q-bio Summer School on Cellular Information Processing, which was sponsored by the New Mexico Consortium's Institute for Advanced Studies, and the Center for Nonlinear Studies at Los Alamos National Laboratory.

* Present address: Center for Cell Analysis and Modeling, University of Connecticut Health Center, Farmington, CT, 06030, USA.

† Corresponding author: mewall@lanl.gov

[1] A. Novick and M. Weiner, Proc Natl Acad Sci USA **43**, 553 (1957).

[2] E. M. Ozbudak, M. Thattai, H. N. Lim, B. I. Shraiman, and A. Van Oudenaarden, Nature **427**, 737 (2004).

[3] M. A. Savageau, Chaos **11**, 142 (2001).

[4] M. A. Savageau, Math Biosci **180**, 237 (2002).

[5] N. Yildirim and M. C. Mackey, Biophys J **84**, 2841 (2003).

[6] N. Yildirim, M. Santillan, D. Horike, and M. C. Mackey, Chaos **14**, 279 (2004).

[7] M. J. van Hoek and P. Hogeweg, Biophys J **91**, 2833 (2006).

[8] A. Narang and S. S. Pilyugin, Bull Math Biol **70**, 1032 (2008).

[9] M. van Hoek and P. Hogeweg, PLoS Comput Biol **3**, e111 (2007).

[10] M. Santillan, M. C. Mackey, and E. S. Zeron, Biophys J **92**, 3830 (2007).

[11] J. T. Mettetal, D. Muzzey, J. M. Pedraza, E. M. Ozbudak, and A. van Oudenaarden, Proc Natl Acad Sci U S A **103**, 7304 (2006).

[12] J. S. Lolkema, N. Carrasco, and H. R. Kaback, Biochemistry **30**, 1284 (1991).

[13] J. Abramson, I. Smirnova, V. Kasho, G. Verner, H. R. Kaback, and S. Iwata, Science **301**, 610 (2003).

[14] L. Guan, O. Mirza, G. Verner, S. Iwata, and H. R. Kaback, Proc Natl Acad Sci U S A **104**, 15294 (2007).

[15] B. Magasanik and F. C. Neidhardt, in *Escherichia coli and Salmonella typhimurium: Cellular and Molecular Biology*, edited by F. C. Neidhardt (American Society for Microbiology, Washington, DC, 1987), vol. 2, pp. 1318–1325, 1st ed.

[16] P. Wong, S. Gladney, and J. D. Keasling, Biotechnol Prog **13**, 132 (1997).

[17] A. Narang, J Theor Biol **247**, 695 (2007).

[18] J. M. Vilar, C. C. Guet, and S. Leibler, J Cell Biol **161**, 471 (2003).

[19] P. C. Maloney and T. H. Wilson, Biochim Biophys Acta **330**, 196 (1973).

[20] F. Kepes, Biochimie **67**, 69 (1985).

[21] J. K. Wright, R. Seckler, and P. Overath, Annu Rev Biochem **55**, 225 (1986).

[22] P. Viitanen, M. L. Garcia, and H. R. Kaback, Proc Natl Acad Sci U S A **81**, 1629 (1984).

[23] E. P. Kennedy, in *The lactose operon*, edited by J. R. Beckwith and D. Zipser (Cold Spring Harbor Laboratory, Cold Spring Harbor, NY, 1970), pp. 49–92.

[24] J. K. Wright, I. Riede, and P. Overath, Biochemistry **20**, 6404 (1981).

[25] M. G. Page and I. C. West, Biochem J **223**, 723 (1984).

[26] R. E. Huber, G. Kurz, and K. Wallenfels, Biochemistry **15**, 1994 (1976).

[27] M. Martinez-Bilbao, R. E. Holdsworth, L. A. Edwards, and R. E. Huber, J Biol Chem **266**, 4979 (1991).

[28] R. E. Huber, K. Wallenfels, and G. Kurz, Can J Biochem **53**, 1035 (1975).

[29] D. Kennell and H. Riezman, J Mol Biol **114**, 1 (1977).

[30] H. E. Kubitschek and J. A. Friske, J Bacteriol **168**, 1466 (1986).

[31] H. E. Kubitschek, J Bacteriol **172**, 94 (1990).

[32] J. Beckwith, in *Escherichia coli and Salmonella typhimurium: Cellular and Molecular Biology*, edited by F. C. Neidhardt (American Society for Microbiology, Washington, DC, 1987), vol. 2, pp. 1444–1452, 1st ed.

[33] J. R. Sadler and A. Novick, J Mol Biol **12**, 305 (1965).

[34] G. Yagil and E. Yagil, Biophys J **11**, 11 (1971).

[35] M. Cohn and K. Horibata, J Bacteriol **78**, 613 (1959).

[36] M. E. Wall, M. J. Dunlop, and W. S. Hlavacek, J Mol Biol **349**, 501 (2005).